FRESNEL RAYS AND RESOLUTION OF TOMOGRAPHIC IMAGING

Claudio Chiaruttini
D.I.N.M.A., University of Trieste, via Valerio, 10, I-34127 Trieste, Italy
tel: +39 40 676 7157; fax: +39 40 676 3497
e-mail: chiaruttini@univ.trieste.it
Alessandro Pregarz and *Enrico Priolo*
Osservatorio Geofisico Sperimentale (OGS), Trieste, Italy

ABSTRACT

Ray-theoretic travel-time tomography assumes an infinite signal bandwidth. When this condition is not met, energy propagates from source to receiver along Fresnel rays of finite cross-section, instead of infinitely thin mathematical rays. We use approximate analytical solutions of the weak scattering problem and numerical modelling of the full wave equation to discuss the resolution of bandlimited records. The setting of the numerical simulations is illustrative of a cross-well seismic experiment. We show that bandlimited travel-time data suffer an unexpected loss of resolution just along the mathematical ray. Nevertheless, this loss can be fully recovered including signal amplitude in an inversion procedure. We also discuss the problem of time picking, and show that, to be consistent with the weak scattering assumption, arrival time must be estimated at the signal peak.

1 INTRODUCTION

The principles of travel-time tomography are stated in the time domain and are valid asymptotically in the high frequency limit. It is well known that the high-frequency condition—meaning that the perturbed slowness is almost constant in a signal wavelength—is usually not met in experimental settings of great industrial importance, like seismic exploration [2] and ground penetrating radar. Wave propagation phenomena can be handled by diffraction tomography [1], which is stated in the frequency domain. Recently, Rocca and Woodward merged these two approaches introducing the wave equation-tomography, which is stated in the time domain and includes diffraction [7, 8]. This theory allows a deep insight into the resolving power of band-limited travel-time data.

Following Woodward and Rocca, we use the Rytov approximation of the scattered wavefield to define the Fresnel rays, volumes of finite cross-section over which bandlimited energy propagates, and use them to investigate the resolution of real signals. The analytical conclusions are validated with a numerical spectral element modelling of the full wave equation.

We show that travel-time data have an unexpected loss of resolution just along the shortest travel-path (mathematical ray). Nevertheless, this loss can be fully recovered including signal amplitude in an inversion procedure.

Wave-equation tomography defines delays from the phase spectrum, in the non-dispersive assumption that scattering does not distort the signal. As this is not the practical case, a question arises on the existence of a signal feature in the time domain, if any, which is mostly representative of the theoretically predicted delays. By means of numerical modelling, we show that this feature is the signal peak.

2 ANALYTICAL DISCUSSION

2.1 Mathematical rays

In travel-time tomography, the unknown velocity field can be recovered from measurements of wave arrival-times through the following integral equation:

$$t(\mathbf{g};\mathbf{s}) = \int w(\mathbf{r})\, L[\mathbf{r};\mathbf{s},\mathbf{g},w(\mathbf{r})]\, d\mathbf{r}, \qquad (1)$$

where t is the travel-time between the source $\mathbf{s}$ and the receiver (geophone) $\mathbf{g}$, $\mathbf{r}$ is the position vector, $w = 1/c$ is the slowness (reciprocal of velocity) in the medium, L is a distribution representing the raypath—i.e., $+\infty$ along the ray, 0 elsewhere. This equation is nonlinear in w, since it appears both as a factor in the integrand and as an argument of L. If we decompose the unknown slowness field into a known background field w_0 plus a small perturbation Δw, equation (1) can be linearized as:

$$\Delta t(\mathbf{g};\mathbf{s}) = \int \Delta w(\mathbf{r})\, L_0[\mathbf{r};\mathbf{s},\mathbf{g},w_0(\mathbf{r})]\, d\mathbf{r}, \qquad (2)$$

where Δt is the time delay of the observed signal with respect to the travel-time t_0 in the background medium. This expression is a generalized Radon transform, meaning that the unknown perturbed velocity field is sampled with line integral projections over unperturbed raypaths L_0. The unknown field Δw is recovered backprojecting delays over the mathematical raypaths [3].

2.2 Monochromatic wavepaths

When ray-theoretic hypotheses are not valid, the full wave equation has to be considered. Under some limiting assumptions, a wave-theoretic equivalent to equation (2) can be obtained by linearizing the scalar wave equation according to Rytov method [8].

The Rytov approximation is based on the representation of the wavefield Ψ by an exponential with complex argument: $\Psi = \exp(\Phi)$. In such a way, the real part of Φ accounts for the wave amplitude, and the imaginary part for the phase, which is directly related to travel-time. Under the weak (or single) scattering assumption, the approximate solution for a given angular frequency ω can be written as:

$$\Delta\Phi(\omega, \mathbf{g}; \mathbf{s}) = \int \frac{\Delta c(\mathbf{r})}{c_0(\mathbf{r})} \mathcal{L}_0(\omega, \mathbf{r}; \mathbf{s}, \mathbf{g})\, d\mathbf{r}, \tag{3}$$

where $\Delta\Phi$ is the scattered wavefield, c_0 is the background velocity, and Δc is the velocity perturbation. Due to the formal analogy between equations (2) and (3), Woodward calls the kernel $\mathcal{L}_0$ the Rytov "wavepath"; its properties control the resolution of wave-theoretic tomography. The validity condition for Rytov approximation is that of a small change of the wavefield over a wavelength.

2.3 Fresnel rays

A long observation time is necessary for the precise determination of phase shifts. To reconcile wave-theoretic tomography with time-delay tomography, Woodward [8] transforms phase perturbation to time delay through the map $\Delta t = \Im[\Delta\Phi]/\omega$, and averaging over the frequency band. Extending Woodward's approach to a generic spectrum $\mathcal{F}(\omega)$, we write [5] the time-delay as:

$$\Delta t = \int_0^\infty \mathcal{P}(\omega) \frac{\Im[\Delta\Phi(\omega)]}{\omega}\, d\omega, \tag{4}$$

where $\mathcal{P}(\omega)$ is the normalized power spectrum of the unperturbed signal, given by

$$\mathcal{P}(\omega) = \frac{|\mathcal{F}(\omega)|^2}{\int_0^\infty |\mathcal{F}(\omega)|^2 d\omega}. \tag{5}$$

For a constant energy spectrum with bandwidth $\Delta\omega = \omega_2 - \omega_1$, equation (5) reduces to $1/\Delta\omega$.

Using equation (3), it is convenient to write equation (4) as:

$$\Delta t = \int \frac{\Delta c(\mathbf{r})}{c_0(\mathbf{r})} L_{\mathcal{P}(\omega)}(\mathbf{r})\, d\mathbf{r}, \tag{6}$$

where

$$L_{\mathcal{P}(\omega)}(\mathbf{r}) = \int_0^\infty \mathcal{P}(\omega) \frac{\Im[\mathcal{L}_0(\omega, \mathbf{r})]}{\omega}\, d\omega \tag{7}$$

is the Fresnel ray (or "bandlimited raypath"), which determines the resolution bandlimited travel-time tomography. Equation (7) is the backprojection pattern corresponding to the given bandlimited signal [7, 8].

Velocity anomalies not only produce time delays, they affect the amplitude of the wavefield as well. Recognizing that the real part of $\Delta\Phi$ is the rate of amplitude change in the frequency domain $(|\Psi| - |\Psi_0|)/|\Psi_0|$, we estimate the overall scattering amplitude rate Δa in the frequency band by averaging the real part of $\Delta\Phi$ over the signal spectrum:

$$\Delta a = \int_0^\infty \mathcal{P}(\omega) \Re[\Delta\Phi(\omega)]\, d\omega, \tag{8}$$

which we write as:

$$\Delta a = \int \frac{\Delta c(\mathbf{r})}{c_0(\mathbf{r})} A_{\mathcal{P}(\omega)}(\mathbf{r})\, d\mathbf{r}, \tag{9}$$

with

$$A_{\mathcal{P}(\omega)}(\mathbf{r}) = \int_0^\infty \mathcal{P}(\omega) \Re[\mathcal{L}_0(\omega, \mathbf{r})]\, d\omega. \tag{10}$$

For instance, for a point source in a 3-D space and a constant spectrum (box-car function), the formal integration of (7) and (10) [5] leads respectively to

$$\begin{aligned} L_{\Delta\omega}(\mathbf{r}) &= \frac{1}{2\pi\Delta\omega[c_0\tau(\mathbf{r})]^2} \frac{|\mathbf{g}-\mathbf{s}|}{|\mathbf{r}-\mathbf{g}||\mathbf{r}-\mathbf{s}|} \\ &\quad \Big[\sin(\omega\,\tau(\mathbf{r})) - \omega\,\tau(\mathbf{r})\,\cos(\omega\,\tau(\mathbf{r}))\Big]_{\omega_1}^{\omega_2} \end{aligned} \tag{11}$$

and

$$\begin{aligned} A_{\Delta\omega}(\mathbf{r}) &= \frac{1}{2\pi\Delta\omega c_0^2\tau^3(\mathbf{r})} \frac{|\mathbf{g}-\mathbf{s}|}{|\mathbf{r}-\mathbf{g}||\mathbf{r}-\mathbf{s}|} \big[(\omega^2\tau^2(\mathbf{r}) - 2) \\ &\quad \sin(\omega\tau(\mathbf{r})) + 2\omega\tau(\mathbf{r})\cos(\omega\tau(\mathbf{r}))\big]_{\omega_1}^{\omega_2}, \end{aligned} \tag{12}$$

where $\tau(\mathbf{r}; \mathbf{s}, \mathbf{g}) = (|\mathbf{r}-\mathbf{s}| + |\mathbf{r}-\mathbf{g}| - |\mathbf{g}-\mathbf{s}|)/c_0$ is the diffraction delay.

Similarly, for a point source in a 2-D space (3-D line source), the kernels of the integrals (6) and (9) are:

$$\begin{aligned} L_{\Delta\omega}(\mathbf{r}) &= \frac{-1}{2\Delta\omega\sqrt{2}[c_0\tau(\mathbf{r})]^{\frac{3}{2}}} \sqrt{\frac{|\mathbf{g}-\mathbf{s}|}{|\mathbf{r}-\mathbf{g}||\mathbf{r}-\mathbf{s}|}} \\ &\quad \left[2\sqrt{\frac{\omega\tau(\mathbf{r})}{\pi}}\cos\Big(\omega\tau(\mathbf{r}) + \frac{\pi}{4}\Big) - \right. \\ &\quad \left. C\left(\sqrt{\frac{2\,\omega\tau(\mathbf{r})}{\pi}}\right) + S\left(\sqrt{\frac{2\,\omega\tau(\mathbf{r})}{\pi}}\right)\right]_{\omega_1}^{\omega_2} \end{aligned} \tag{13}$$

and

$$\begin{aligned} A_{\Delta\omega}(\mathbf{r}) &= \frac{3}{4\Delta\omega\sqrt{2c_0^3\tau^5(\mathbf{r})}} \sqrt{\frac{|\mathbf{g}-\mathbf{s}|}{|\mathbf{r}-\mathbf{g}||\mathbf{r}-\mathbf{s}|}} \\ &\quad \left[\frac{4\pi}{3}\left(\frac{\omega\tau(\mathbf{r})}{\pi}\right)^{\frac{3}{2}}\sin\Big(\omega\tau(\mathbf{r}) + \frac{\pi}{4}\Big) + \right. \\ &\quad 2\sqrt{\frac{\omega\tau(\mathbf{r})}{\pi}}\cos\Big(\omega\tau(\mathbf{r}) + \frac{\pi}{4}\Big) - \\ &\quad \left. C\left(\sqrt{\frac{2\,\omega\tau(\mathbf{r})}{\pi}}\right) + S\left(\sqrt{\frac{2\,\omega\tau(\mathbf{r})}{\pi}}\right)\right]_{\omega_1}^{\omega_2}, \end{aligned} \tag{14}$$

where C and S are the Fresnel integrals.
Fresnel rays (Fig. 1) are the physical volumes through which energy propagates from source to receiver. They have an oscillatory nature, with a characteristic length equal to the first Fresnel radius:

$$R_F = \frac{1}{2}\sqrt{\frac{2\pi}{\omega_c}\,\mathsf{L}}, \tag{15}$$

where ω_c is the signal dominant frequency, and L is the source-receiver distance. It comes out that an object much smaller than R_F can produce either positive or

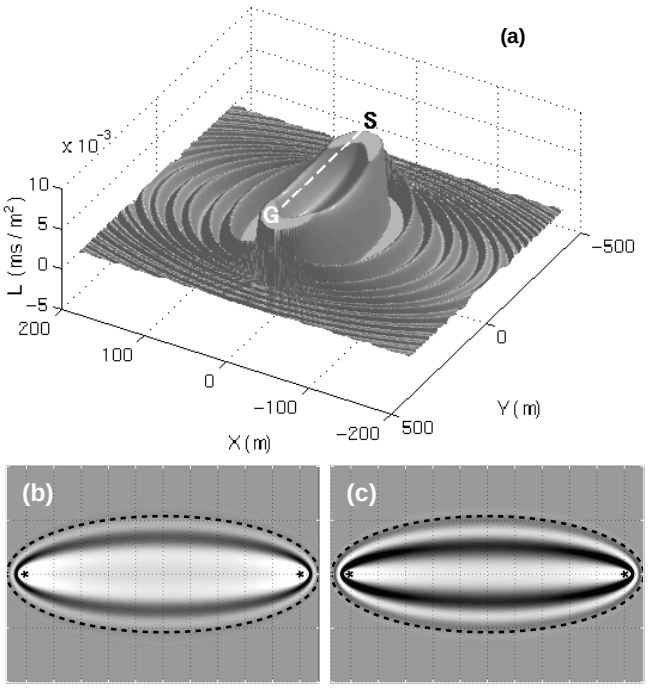

Figure 1: Fresnel rays. (a) 3-D view of 2-D time delay; the signal has a uniform energy distribution within the band 0–200 Hz. (b) Map of 2-D time delay and (c) amplitude perturbation; the signal is a Ricker wavelet with energy within the band 0–200 Hz. The dashed line in (b) and (c) is the Fresnel ray edge. For all pictures, the medium is homogeneous with $c_0 = 3000$ m/s, and $\mathsf{L} = 519.2$ m.

negative time/amplitude changes, depending on its location within the positive or negative lobes of the raypath. Therefore, in the tomographic reconstruction of a small object, a sign ambiguity is to be expected in addition to the impossibility of recovering its size. Woodward [8] shows that the resolution of a bandlimited wavefield is estimated by the width of the raypath envelope, called "bandlimited ray-width". At half the source-receiver distance, this quantity is approximated by

$$R_{\Delta\omega} = \sqrt{\frac{\pi c}{\Delta\omega}\left(\frac{\pi c}{\Delta\omega} + \mathsf{L}\right)}, \tag{16}$$

where $\Delta\omega$ is a measure of the signal bandwidth. The bandlimited ray-width is inversely dependent on the frequency bandwidth, and does not depend on the central frequency of the signal. A sharp frequency cut-off produces ripples slowly decaying with distance, in much the same way as spectral truncation produces the Gibb's effect in the inverse Fourier transform (Fig. 1a). On the contrary, smooth amplitude spectra result in patterns almost totally confined within $R_{\Delta\omega}$ (Fig. 1b-c). For such signals, it is possible to define an equivalent bandwidth, with constant spectral energy level therein, which closely reproduces the bandlimited raypath within its width $R_{\Delta\omega}$ [5].
Contrasting with ray-theory, Fresnel rays predict that the greatest time delay is achieved by diffractors placed at some distance from the mathematical ray (Fig. 2). This effect is striking in the 3-D case, where a small scatterer placed on the shortest-time path would produce no delay at all, and therefore could not be detected by travel-time analysis. A similar loss of resolution is found also in 2-D media, although a partial time delay is now observable for a scatterer lying on the ray. This unexpected effect is an outcome of the single scattering condition [5]. 2-D and 3-D Fresnel rays share the property that amplitude variation and time delay are nearly in quadrature. This means that time and amplitude carry independent and complementary information: what is missing in time is found in amplitude, and vice-versa.

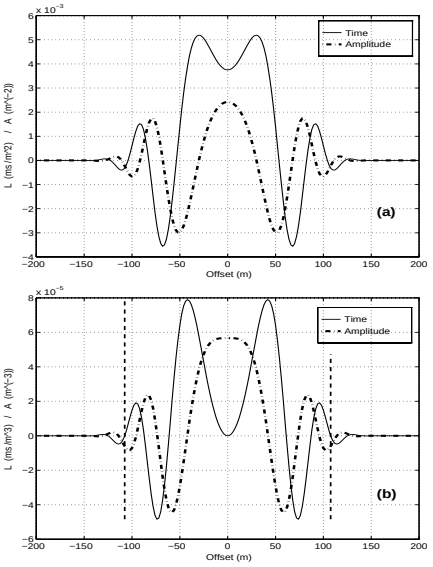

Figure 2:
(a) Time delay and amplitude perturbation ratio on a cross-section of the 2-D Fresnel ray at half the source-receiver distance.
(b) The same for 3-D. Vertical dashed lines indicate the ray edges. Same model as Fig. 1. The signal is a Ricker wavelet.

Finally, wave-equation tomography derives time delay from the phase spectrum (equation (4)), with no obvious relation to any time-domain picking method (for instance, at first break or at signal peak). This topic—of utmost importance when dealing with real data—is further investigated by numerical modelling.

3 NUMERICAL EXPERIMENTS

We use spectral element modelling (SPEM) [6] of the full wave equation to confirm the analytical discussion and to compare results obtained using different methods of

time picking. The simulations reproduce a seismic cross-well experiment with bandlimited energy, and consist of a family of 2-D acoustic models where a narrow velocity perturbation parallel to the mathematical ray is located at different offsets from it [5]. The source-receiver distance is $\mathsf{L} = 519.2$ m and the velocity of the background medium is $c_0 = 3000$ m/s. The perturbation is a rectangle 138.4×13 m^2 in size, with velocity $c = 3100$ m/s. The source time history is a Ricker wavelet with a central frequency $F_c = 100$ Hz (maximum frequency $2F_c$), resulting in a dominating wavelength $\lambda = 30$ m and an equivalent bandwidth of 65–135 Hz. The bandlimited ray-width is $R_{\Delta\omega} \approx 107$ m. For the same energy spectrum, we used two different time histories, namely a zero- and a minimum-phase wavelet: the first is widely used in numerical modelling, the second is more representative of a real seismic or radar pulse. Our conclusions are valid for both signal shapes [4, 5].

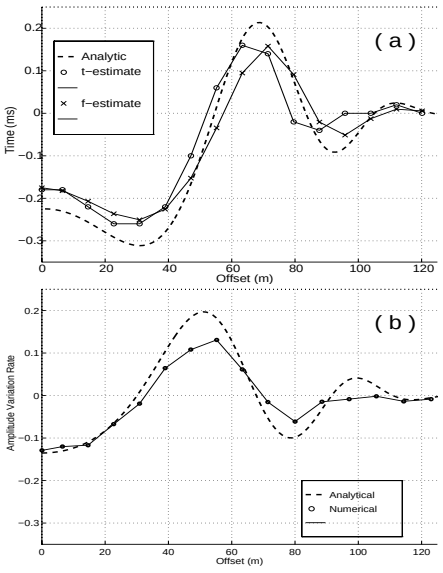

Figure 3: Comparison of analytical and numerical values of: (a) time delay, and (b) amplitude perturbation ratio, versus offset for the 2-D model. Circles indicate estimates in the time domain; crosses, estimates in the frequency domain.

Figure 3 shows that the agreement between numerical and theoretical estimates is pretty good, if we estimate both delay and amplitude at the signal peak in the time domain. Although impractical, time delay results correct also when estimated in the frequency domain, by the formula $\Delta t = \int_0^\infty \mathcal{P}(\omega)[\Delta\phi(\omega)/\omega]\, d\omega$, where $\Delta\phi(\omega)$ is the scattered phase spectrum. The oscillating character of both curves is accurately reconstructed, and experimental delays do present a local maximum at offset zero. In general, experimental data slightly underestimate the theoretical predictions. Attempts to pick time at the first break, or by correlation with the unperturbed signal, produced results inconsistent with the theory [4, 5].

4 CONCLUSION

We investigated in detail, by analytical and numerical means, how the scattered wavefield depends on the offset from the mathematical ray of a small and localized velocity anomaly. Our analysis shows that, to be consistent with the single scattering assumption of wave-equation tomography, the arrival-time should be estimated at the peak value, as the signal amplitude actually is. Let us incidentally note that, on the contrary, ray-theory assumes multiple scattering, thus requiring time picking at first break. We showed also that the amount of information carried by travel-time data is unexpectedly low in correspondence of the shortest travel-path. This information is completely lost in 3-D, and only partially in 2-D. Nevertheless, it can be fully recovered using signal amplitude. Therefore, both travel-time and amplitude should be inverted for optimal exploitation of experimental data.

Finally, for bandlimited signals with a smooth energy distribution, the raypath is definitely confined within the bandlimited ray-width. Outside of it, signals with sharp cut-off show a slowly decaying ringing that closely reflects the well known Gibb's phenomenon of spectral truncation.

ACKNOWLEDGMENTS

This research was partly funded by the European Union (Contracts JOU2-CT92-0096, and JOU2-CT93-0321).

References

[1] Devaney, A. J., 1982. A filtered backpropagation algorithm for diffraction tomography, *Ultrasonic Imaging*, **4**, 336–350.

[2] Hagedoorn, J. G., 1959. A process of seismic reflection interpretation, *Geophysical Prospecting*, **2**, 85–127.

[3] Nolet, G., 1987. Seismic wave propagation and seismic tomography, in G. Nolet, ed.: *Seismic Tomography,* Reidel, pp. 1–23.

[4] Priolo, E., C. Chiaruttini, and A. Pregarz, in press. Influence of signal band-limitation on the resolution of travel-time tomography: 2-D numerical experiments, *Proc. 2nd Int. Conf. on Theor. and Comp. Acoust.*, Honolulu (Hawaii), World Scient.

[5] Priolo, E., C. Chiaruttini, and A. Pregarz, 1996. Analytical and numerical analysis of the tomographic resolution with bandlimited signals, submitted to *Geophysics*.

[6] Seriani, G., and E. Priolo, 1991. High-order spectral element method for acoustic wave modeling, *61st Ann. Int. Mtg., Houston, Texas, Soc. Expl. Geophys., Expanded Abstracts,* pp. 1561–1564.

[7] Woodward, M. J., and F. Rocca, 1988. Wave-equation tomography, *58th Ann. Int. Mtg., Anaheim (CA), Soc. Expl. Geophys., Expanded Abstracts,* pp. 1232–1235.

[8] Woodward, M. J., 1992. Wave-equation tomography, *Geophysics*, **57** (1), 15–26.